Proc. Natl. Acad. Sci. USA
Vol. 90, pp. 9066–9069, October 1993
Neurobiology

An interdigitated columnar mosaic of cytochrome oxidase, zinc, and neurotransmitter-related molecules in cat and monkey visual cortex

(serotonin 1C receptor/acetylcholinesterase/cortical columns/histochemistry)

RICHARD H. DYCK* AND MAX S. CYNADER

Department of Ophthalmology, University of British Columbia, Vancouver, BC Canada V5Z 3N9

Communicated by Vernon B. Mountcastle, June 18, 1993

ABSTRACT **There is considerable physiological evidence for the compartmentalization of mammalian visual cortex into functional columnar modules, representing features of visual information processing such as eye and orientation specificity. However, anatomical markers of visual cortical compartmentalization have been described only for primate visual cortex. In this report, we describe an interdigitated mosaic of four neuroactive molecules which demarcate two distinct columnar systems in the kitten visual cortex. Serotonin 1C receptors and synaptic zinc were found to demarcate columns within layer IV of kitten visual cortex, which were interdigitated with a second, patchy system characterized by increased levels of cytochrome oxidase and acetylcholinesterase. In primate visual cortex, as well as in the kitten, synaptic zinc was periodically distributed in a manner precisely complementary to cytochrome oxidase. These findings provide an anatomical framework on which unifying hypotheses of the functional organization of columnar systems in mammalian visual cortex can be built.**

The columnar arrangement of functionally similar elements has long been considered to be a fundamental principle of neocortical organization (1, 2). The demonstration that cytochrome oxidase-enriched blobs overlie eye-specific columns in primate visual cortex (3) has proven to be invaluable in providing an anatomical reference point from which theories regarding the functional compartmentalization of mammalian visual cortex have evolved (reviewed in ref. 4). Since this discovery, the distributions of several enzymes and other molecules associated with the functions of neurotransmitters have been shown to be either coincident with or complementary to cytochrome oxidase blobs in primate visual cortex (4). Unfortunately, cytochrome oxidase blobs were reported to be unique to primates (5, 6), leading to hypotheses which constrained functional relationships of these blobs to features of visual processing also unique to primates. Recent studies, however, indicate the presence of a periodic distribution of cytochrome oxidase in the visual cortex of carnivores (7–9), thus providing an anatomical basis for columnar compartments common to both orders.

The columnar parcellation of visual cortex into eye- and orientation-specific domains emerges in development as a result of input- and activity-dependent interactions between cortical afferents and their postsynaptic targets (10–12). This functional organization can be effectively modified by visual experience during a discrete temporal window of development (13–15). We have recently reported (16, 17) that several anatomical markers of neurotransmitter specific-systems are arranged in a columnar manner in layer IV of striate cortex of cats and might, therefore, participate in the formation and plasticity of its functional organization (16, 17). In this report, we describe the topographical distribution of several neuroactive molecules which demarcate columnar domains in the primary visual cortex of both cats and monkeys. Our identification of multiple markers for a columnar mosaic in mammalian visual cortex provides a rationale for future physiological studies, which will be required to understand the functional importance of this neurochemical organization. A preliminary account of these data has been presented in abstract form (9, 18).

MATERIALS AND METHODS

Animals and Tissue Preparation. Ten kittens between the ages of 50 and 75 days were used in this study. This age range was selected because the columnar expression of zinc and serotonin receptors is maximally defined within this developmental window (16, 17). Ocular dominance columns were visualized autoradiographically in four kittens 12 days after an intraocular injection of [^{3}H]proline (2.0 mCi in 25 μl of saline; NEN; 1 mCi = 37 MBq) (19). The other eye was injected with vehicle alone. All kittens were anesthetized to effect with halothane. The saphenous vein was cannulated, and an intravenous injection of sodium selenite (10 mg/ml in water; 10 mg/kg of body mass) was administered at a rate of 1 ml/min. Following a 15- to 20-min survival period the animals were killed with an overdose of sodium pentobarbital and perfused through the ascending aorta with 100 ml of 0.1 M Sorenson's buffer (pH 7.4). The brain was quickly removed and the visual cortex from each hemisphere was blocked, opened, and flattened. The tissue blocks were quickly frozen in isopentane and cooled to −50°C on a bed of dry ice. Sections were cut at a thickness of 20 μm on a cryostat at −20°C, thaw-mounted on gelatin-coated glass slides, and stored dessicated at −30°C.

Two adult vervet monkeys (*Cercopithicus aethiops*) were heavily sedated with ketamine and slowly administered an intravenous injection of sodium selenite (10 mg/ml in water; 10 mg/kg of body mass). After 15 min, the monkeys were administered an overdose of sodium pentobarbital and perfused transcardially with 0.1 M Sorenson's buffer (pH 7.4). The brain was quickly removed and the visual operculum from one hemisphere was dissected and flattened between glass slides in order to cut sections tangential to the cortical surface. The other hemisphere was left intact for coronal sections. All tissue blocks were quickly frozen in isopentane (−50°C). Prior to sectioning, pin holes were placed in the flattened hemisphere to provide fiducial landmarks facilitating section alignment and reconstruction. Sections were cut on a cryostat (−20°C), at a thickness of 25 μm, and thaw-mounted on gelatin-coated slides.

Serotonin Receptor Autoradiography. The procedures used to visualize serotonin 1C receptors have been described in detail (16). Briefly, tissue sections were preincubated for 30

The publication costs of this article were defrayed in part by page charge payment. This article must therefore be hereby marked "*advertisement*" in accordance with 18 U.S.C. §1734 solely to indicate this fact.

*To whom reprint requests should be addressed at: Department of Ophthalmology, University of British Columbia, 2550 Willow Street, Vancouver, BC, Canada V5Z 3N9.

min in 170 mM Tris·HCl, pH 7.4/4 mM calcium chloride/5 μM spiperone/10 μM pargylline/0.01% ascorbic acid and then incubated for 120 min in the same buffer containing 4.5 nM [^{3}H]mesulergine (Amersham) to label serotonin 1C sites. The specificity of [^{3}H]mesulergine binding to the serotonin 1C receptor subtype has been characterized previously (20, 21). Nonspecific binding was assessed in near adjacent sections which were processed identically, except that 10 μM serotonin was added to the incubation solution as a nonradioactive displacer. Following incubation, the sections were washed twice for 10 min each in ice-cold buffer and then dried under a cold stream of air. The sections were then apposed, along with ^{3}H standards, to radiation-sensitive film (Hyperfilm; Amersham) and exposed for 10 weeks, to visualize [^{3}H]mesulergine binding.

Cytochrome Oxidase Histochemistry. Cytochrome oxidase was visualized by a modification of the method developed by Wong-Riley (22). This modification, which employed nickel enhancement of the 3,3′-diaminobenzidine reaction product, allowed us to routinely demarcate cytochrome oxidase blobs in cat visual cortex. Prior to staining, sections were fixed for 5 min in 4% paraformaldehyde in 0.05 M phosphate buffer (pH 7.4) and then rinsed for 5 min in buffer only. The sections were incubated (37°C, 30–60 min) in a reaction medium consisting of 1 g of sucrose, 50 mg of nickel ammonium sulfate, 25 mg 3,3′-diaminobenzidine, 15 mg of cytochrome *c*, 10 mg of catalase, and 250 μl of 1.0 M imidazole in 100 ml of 0.05 M phosphate buffer (pH 7.4). The reaction was stopped by rinsing in the buffer solution for 10 min.

Zinc Histochemistry. Synaptic zinc was visualized by physical development as described (17). Briefly, slide-mounted tissue sections were fixed in ethanol, coated with 0.5% gelatin, and then incubated in 200 ml of freshly prepared developer containing 120 ml of 50% gum arabic, 20 ml of 2.0 M sodium citrate buffer, 30 ml of 0.5 M hydroquinone and 30 ml of 37 mM silver lactate. In complete darkness, sections were incubated in the developing solution at 26°C for 100–150 min.

Acetylcholinesterase Histochemistry. Sections intended for the detection of acetylcholinesterase were fixed in 4% paraformaldehyde in 0.05 M phosphate buffer (pH 7.4) for 10 min and then rinsed in buffer. The staining procedure was as described by Karnovsky and Roots (23). The fixed sections were preincubated for 30 min in phosphate buffer containing 30 μM tetraisopropylpyrophosphoramide to inhibit butyrylcholinesterase activity. The cholinesterase-positive reaction was visualized following incubation for 3-4 hr (at room temperature) in 300 ml of 50 mM Tris maleate buffer (pH 6.0) containing 150 mg of acetylthiocholine iodide, 441 mg of sodium citrate, 225 mg of cupric sulfate, and 49 mg of potassium ferricyanide.

Digital Imaging. Histochemically stained sections and autoradiographic images were digitally captured and aligned by using a CCD camera (4915; Cohu, San Diego) and a framegrabber card (DT-2255; Data Translation, Marlboro, MA) installed in a Macintosh IIfx computer running NIH IMAGE software. Coincidence or complementarity of neurochemical markers was ascertained by using the merge and arithmetic features of ADOBE PHOTOSHOP (Adobe Systems, Mountain View, CA).

RESULTS AND DISCUSSION

Using *in vitro* autoradiographic methods, we found that the serotonin 1C receptor subtype was expressed in columns within layer IV of kitten visual cortical area 17 only between 4 and 12 weeks postnatally (16). The periodic pattern of serotonin 1C receptors labeled with [^{3}H]mesulergine is shown in coronal (Fig. 1*A*) and tangential (Fig. 1*B*) planes through the visual cortex of a 50-day-old kitten. Patches of

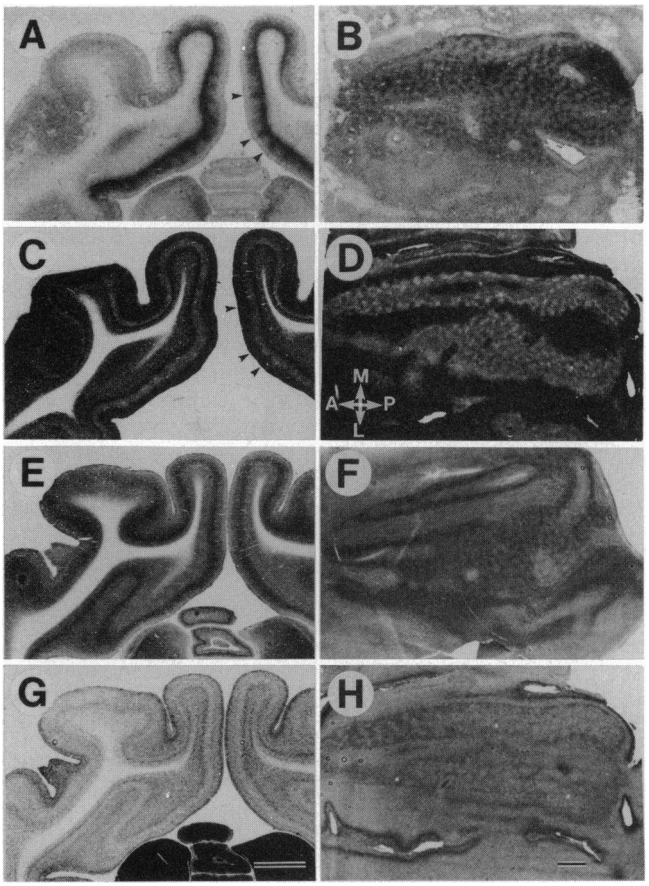

FIG. 1. Multiplicity of markers for columnar domains in kitten visual cortex at postnatal day 50. The columnar distributions of serotonin 1C receptors (*A* and *B*) and synaptic zinc (*C* and *D*) in layer IV of area 17 were apparent even in the frontal plane (*A* and *C*). The registration of several columns was apparent in the frontal plane (arrowheads). The distributions of cytochrome oxidase (*E* and *F*) and acetylcholinesterase (*G* and *H*), which were also cytochemical markers of the columnar architecture in primate striate cortex, did not appear patchy in frontal sections (*E* and *F*) but clearly demarcated columnar domains in the tangential plane (*F* and *H*). Although the most marked columnar distribution of each of the four markers was found in different layer IV substrata, their organization into patches of increased density all exhibited the same periodicity in area 17 (center-to-center distance, 900–1000 μm). Directions in *D*: A, anterior; P, posterior; M, medial; L, lateral. (Bars = 3.0 mm.)

increased receptor density, ≈400 μm in diameter, were found to be distributed in layer IV, throughout area 17, with an average center-to-center spacing of 900–1000 μm.

The distribution of zinc, which is enriched in a subset of glutamatergic terminals (24, 25), also exhibited column-specific labeling in layer IV of area 17 of kitten visual cortex (17). In coronal (Fig. 1*C*) and tangential (Fig. 1*D*) sections through visual cortex of 50-day-old kittens, the distribution of zinc was densest, and homogeneous, in layers I–III and V. The patchy distribution of zinc was visible in layer IV in the coronal plane (Fig. 1*C*, arrowheads) but was much more obvious in sections cut tangential to the cortical surface (Fig. 1*D*). When compared with the distribution of serotonin 1C receptors in a serially adjacent section, patches of increased levels of zinc and serotonin 1C receptors were found to be precisely overlapped and localized to the same vertical column (Fig. 1 *A* and *C*; note arrowheads).

We compared the distribution of these markers with that of cytochrome oxidase in serially adjacent sections. As in the adult cat (8), the patchy distribution of cytochrome oxidase in 50-day-old kittens was not readily apparent in coronal

sections (Fig. 1*E*) but was clear in the tangential plane (Fig. 1*F*). We also found acetylcholinesterase to exhibit a periodic pattern in tangential sections (Fig. 1*H*), which was not apparent in the coronal plane (Fig. 1*G*). Acetylcholinesterase-rich patches were limited to a thin band at the layer III/IV border (Fig. 1*H*); those patches were aligned with cytochrome oxidase blobs but complementary to zinc/serotonin 1C receptor columns (data not shown). The complementary relationship between cytochrome oxidase/acetylcholinesterase-enriched blobs and the zinc/serotonin 1C receptor patches in layer IV can be seen in Fig. 2. Digitally captured images showing the patchy distribution of cytochrome oxidase (Fig. 2*A*) and zinc (Fig. 2*B*) are shown individually and then are superimposed and summed (Fig. 2 *C* and *D*). The homogeneous image resulting from the summation of carefully aligned zinc- and cytochrome oxidase-stained sections (Fig. 2*C*) contrasted with the reappearance of the distinct periodicity when the overlying image was shifted to the right by a distance equal to half of the average patch spacing (450 μm) and then summed (Fig. 2*D*), indicating that these two systems were precisely complementary in the tangential domain.

The distributions of several enzymes and other molecules associated with the functions of neurotransmitters have been shown to be either aligned with or complementary to cytochrome oxidase blobs in primate visual cortex (4). These data, and those reported here, suggest that column-specific molecules might demarcate common functional domains in the visual cortex of phylogenetic orders as diverse as carnivores and primates. Indeed, we found that the laminar-specific distribution of zinc (Fig. 3 *B*, *D*, and *G*) in striate cortex of adult primates (*C. aethiops*) was exactly complementary to that of cytochrome oxidase (Fig. 3 *A*, *C*, and *F*), just as it was in the cat. In the tangential plane of section,

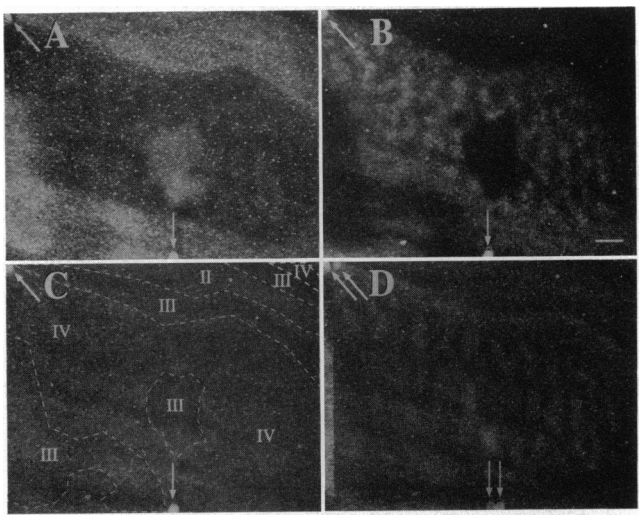

FIG. 2. High-magnification digital images of cytochrome oxidase (*A*) and zinc (*B*) staining in serially adjacent sections through area 17 of kitten visual cortex at postnatal day 50. The periodic, patchy distributions of both cytochrome oxidase and synaptic zinc are evident in layer IV. When the two sections were superimposed and summed, the precise laminar and columnar complementarity of these two markers was manifested by the disappearance of the patchy pattern in layer IV (*C*). Only the microtome blade scratches showed an increased density following their spatial summation (*C*, diagonal streaks). When the overlying cytochrome oxidase image was shifted to the right by 450 μm and then summed (*D*), the patchy pattern reappeared, indicating that synaptic zinc and cytochrome oxidase are distributed with precise laminar and intralaminar complementarity. White arrows indicate fiducial landmarks used for section alignment. The dotted lines and Roman numerals in *C* outline and indicate laminar boundaries. (Bar = 1 mm.)

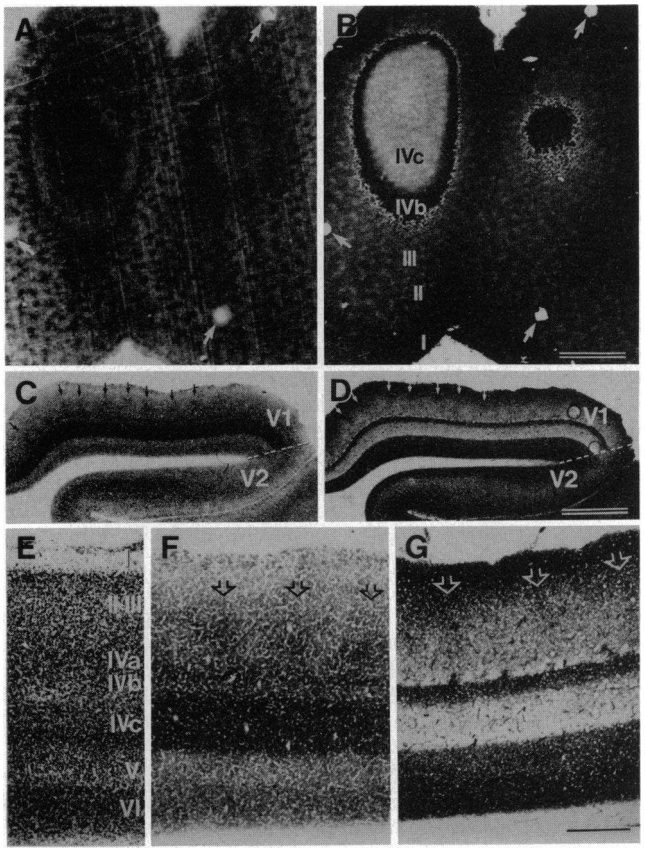

FIG. 3. The distribution of cytochrome oxidase (*A*, *C*, and *F*) and synaptic zinc (*B*, *D*, and *G*) in striate cortex of an adult vervet monkey. The precise complementarity of cytochrome oxidase blobs within a zinc-stained matrix in laminae II/III of V1 was clearly seen in the near-adjacent sections which were cut tangential to the cortical surface (*A* and *B*). The complementary relationship was maintained in lamina IVa, but in this layer, zinc-stained blobs were, instead, surrounded by a cytochrome oxidase matrix. The periodic patterns of cytochrome oxidase and zinc were not robust in coronal sections (*C*, *D*, *F*, and *G*; note arrows), but these panels demonstrate that the laminar-specific distributions of these two molecules also exhibited a high degree of complementarity in V1 and V2 (*C* and *D*). In contrast with cytochrome oxidase (*A*, *C*, and *F*), the highest levels of zinc (*B*, *D*, and *G*) were found in layers I, IVb, and VI, while layers II/III and V were moderately stained. Nissl-stained sections (*E*) were used to establish laminar boundaries. The white arrows in *A* and *B* indicate fiducial landmarks, used to facilitate section alignment. Roman numerals in *B* and *E* indicate the relative locations of cortical laminae. [Bars = 2.0 mm (*A–D*) or 500 μm (*E–G*).]

cytochrome oxidase-rich blobs (Fig. 3*A*) were clearly shown to be interdigitated within a zinc-stained matrix (Fig. 3*B*) in layers II and III of primate cortex. This precise complementarity was evident, in the frontal plane, between laminae as well (Fig. 3 *C*, *D*, *F*, and *G*). Our preliminary results indicate that this complementary relationship between zinc and cytochrome oxidase patches in vervet monkeys is present as early as 4 weeks of age. The distribution of serotonin receptors in visual cortex of developing primates has not yet been examined, although previous studies have shown the distribution of serotonergic afferents to be more abundant in interblob zones (26).

In primates, the cytochrome oxidase-rich zones are associated with (*i*) centers of eye dominance columns, (*ii*) areas of high color selectivity, (*iii*) zones of broad orientation selectivity, and (*iv*) preferential input from particular processing streams originating in the lateral geniculate nucleus (4, 27). To begin to examine the cross-species generality of these functional relationships, we compared the distribution

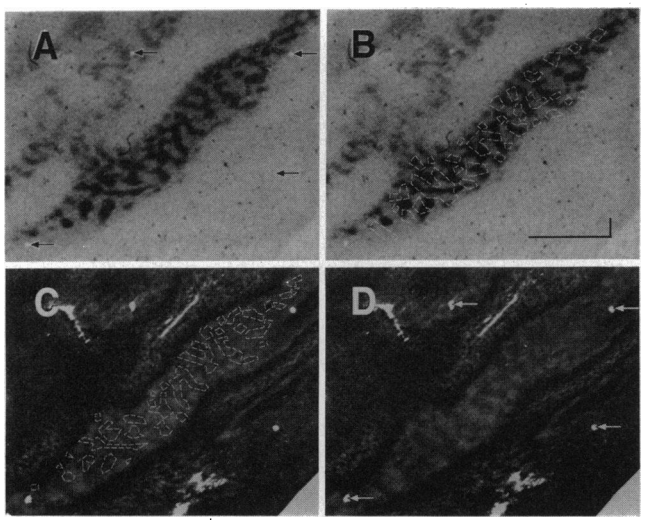

FIG. 4. The relationship between the neurochemically defined columnar architecture in layer IV of kitten visual cortex and ocular dominance columns was determined in the same section stained first for synaptic zinc (*C* and *D*) and then processed for [^{3}H] proline autoradiography (*A* and *B*). In *C*, the outline of the pattern of ipsilateral-eye projections is superimposed on the zinc patches in layer IV, and the zinc-patch outline is superimposed on the ocular dominance distribution in *B*. There does not appear to be an explicit relationship between these columnar systems. Fiducial landmarks used for image alignment are indicated by the arrows in *A* and *D*. (Bars = 4 mm and 1 mm.)

of zinc patches with ocular dominance columns in kitten cortex. Fig. 4 illustrates the tangential distribution of zinc patches (Fig. 4 *C* and *D*), compared with ipsilateral eye-specific patches labeled autoradiographically (Fig. 4 *A* and *B*), in the same section through layer IV of kitten area 17. The dotted lines in Fig. 4*C* indicate the outline of the ocular dominance pattern superimposed on the zinc-stained section, and the outlines of zinc-rich patches are indicated on the ocular dominance map of Fig. 4*B*. Although some overlap between the two patchy patterns was evident, they were not aligned and showed no systematic relationship with one another.

This finding demonstrates that the relationship between the cytochrome oxidase/zinc system and eye-specific innervation observed in primates is not obligatory in cats. Likewise, the association with color is unlikely to be obligatory, given the cat's poor color-vision capacities (28) and the presence of cytochrome oxidase blobs in primates without color vision (29). Our findings are consistent with at least two of the remaining functional interpretations. (*i*) Previous studies have indicated singularities in the cat and monkey cortical orientation maps, zones where different orientation bands coalesce and which contain broadly tuned neurons (30–32). These singularities are thought to be associated with cytochrome oxidase blobs in monkeys (33) and may well have the same association in cat cortex. (*ii*) In primates, the cytochrome oxidase blob/interblob system has been reported to receive geniculate inputs representing different processing streams (4). This is consistent with our findings in kitten striate cortex, which indicate, on the basis of temporal and spatial characteristics of serotonin receptor expression, that 5-serotonin 1C receptors may be preferentially associated with X inputs (ref. 34 and unpublished work).

The results presented here provide anatomical evidence of phylogenetically homologous processing streams in visual cortex. Further studies on the comparative physiology of these columnar systems are needed to determine their precise relationship with the processing of visual information.

We thank A. Chaudhuri for invaluable assistance in obtaining the monkey tissue and for helpful comments regarding the manuscript. We thank N. Swindale for constructive discussion. This work was supported by Medical Research Council of Canada Grant PG 29 (to M.S.C.) and a Natural Sciences and Engineering Research Council postgraduate fellowship (to R.H.D.).

1. Mountcastle, V. B. (1978) in *The Mindful Brain: Cortical Organization and the Group-Selective Theory of Higher Brain Function*, eds. Edelman, G. M. & Mountcastle, V. B. (MIT Press, Boston), pp. 7–50.
2. Lorente de Nó, R. (1949) in *Physiology of the Nervous System*, ed. Fulton, J. F. (Oxford Univ. Press, London), pp. 288–312.
3. Horton, J. C. & Hedley-White, E. T. (1984) *Phil. Trans. R. Soc. London B* **304**, 255–272.
4. LeVay, S. & Nelson, S. B. (1991) in *The Neural Basis of Visual Function*, ed. Leventhal, A. G. (Macmillan, London), pp. 266–315.
5. Horton, J. C. (1984) *Phil. Trans. R. Soc. London B* **304**, 199–253.
6. Horton, J. C. & Hubel, D. H. (1981) *Nature (London)* **292**, 762–764.
7. Cresho, H. S., Rasco, L. M., Rose, G. H. & Condo, G. J. (1992) *Soc. Neurosci. Abstr.* **18**, 298.
8. Murphy, K. M., Van Sluyters, R. C. & Jones, D. G. (1990) *Soc. Neurosci. Abstr.* **16**, 292.
9. Dyck, R. & Cynader, M. (1992) *Soc. Neurosci. Abstr.* **18**, 1308.
10. Stryker, M. P. (1989) *Biomed. Res.* **2**, 37–42.
11. Wiesel, T. N. (1982) *Nature (London)* **299**, 583–588.
12. Löwel, S. & Singer, W. (1992) *Science* **255**, 209–212.
13. LeVay, S., Stryker, M. P. & Shatz, C. J. (1978) *J. Comp. Neurol.* **179**, 223–244.
14. Hubel, D. H. & Wiesel, T. N. (1965) *J. Neurophysiol.* **28**, 1041–1059.
15. Wiesel, T. N. & Hubel, D. H. (1965) *J. Neurophysiol.* **28**, 1029–1040.
16. Dyck, R. H. & Cynader, M. S. (1993) *J. Neurosci.* **13**, 4316–4338.
17. Dyck, R., Beaulieu, C. & Cynader, M. (1993) *J. Comp. Neurol.* **329**, 53–67.
18. Dyck, R. H., Chaudhuri, A. & Cynader, M. S. (1993) *Invest. Ophthalmol. Visual Sci.* **34**, 1173 (abstr.).
19. Wiesel, T. N., Hubel, D. H. & Lam, M.-K. (1974) *Brain Res.* **79**, 273–279.
20. Pazos, A. & Palacios, J. M. (1985) *Brain Res.* **346**, 205–230.
21. Hoyer, D., Pazos, A., Probst, A. & Palacios, J. M. (1986) *Brain Res.* **376**, 97–107.
22. Wong-Riley, M. (1979) *Brain Res.* **171**, 11–28.
23. Karnovsky, M. J. & Roots, L. (1964) *J. Histochem. Cytochem.* **12**, 219–221.
24. Martinez-Guijarro, F. J., Soriano, E., Del Rio, J. A. & Lopez-Garcia, C. (1991) *J. Neurocytol.* **20**, 834–843.
25. Beaulieu, C., Dyck, R. & Cynader, M. (1992) *NeuroReport* **3**, 861–864.
26. Hendrickson, A. E. (1985) *Trends Neurosci.* **8**, 406–410.
27. Livingstone, M. S. & Hubel, D. H. (1988) *Science* **240**, 740–749.
28. Daw, N. W. (1973) *J. Physiol.* **211**, 567–592.
29. Condo, G. J. & Casagrande, V. A. (1990) *J. Comp. Neurol.* **293**, 632–645.
30. Bonhoeffer, T. & Grinvald, A. (1991) *Nature (London)* **353**, 429–431.
31. Blasdel, G. G. & Salama, G. (1986) *Nature (London)* **321**, 579–585.
32. Swindale, N. V., Matsubara, J. A. & Cynader, M. S. (1987) *J. Neurosci.* **7**, 1414–1427.
33. Blasdel, G. G. (1992) *J. Neurosci.* **12**, 3115–3138.
34. Dyck, R. & Cynader, M. (1992) *Invest. Ophthalmol. Visual Sci.* **33**, 1218 (abstr.).